



## Process modeling of brackish and seawater nanofiltration

J. Palmeri<sup>a,\*</sup>, N. Ben Amar<sup>b</sup>, H. Saidani<sup>b,c</sup>, A. Deratani<sup>c</sup>

<sup>a</sup>Université de Toulouse, Université Paul Sabatier, CNRS, Laboratoire de Physique Théorique (IRSAMC); 118 route de Narbonne, 31062 Toulouse Cedex 4, France  
email: john.palmeri@irsamc.ups-tlse.fr

<sup>b</sup>Laboratoire de Modélisation Mathématique et Numérique dans les Sciences de l'Ingénieur, ENIT, Campus Universitaire, B.P 37 Le Belvédère 1002, Tunis, Tunisia

<sup>c</sup>Institut Européen des Membranes, Université Montpellier 2 (ENSCM, UM2, CNRS), 34095 Montpellier cedex 05, France

Received 15 September 2008; Accepted 2 September 2009

### ABSTRACT

We demonstrate that the multi-scale nanofiltration (NF) “process modeling” software, *NanoFlux*, that we are developing can be used to perform reliable desalination plant modeling for highly concentrated brine and seawater feeds in real-world situations.

**Keywords:** Nanofiltration; Modeling; Desalination; Process simulation; Seawater

### 1. Introduction

We have incorporated advanced nanoporous membrane transport models into the multi-scale nanofiltration (NF) “process modeling” software, *NanoFlux*, that we are developing for simulating multi-stage/multi-module NF plants [1–3]. This modeling tool has been used to simulate NF plants in real-world situations and two case studies are presented here for applications concerning the desalination of industrial effluents and seawater (SW):

1. *NF of brackish and highly concentrated brines (textile effluent, Tunisia)* [4];
2. *Seawater NF (SWNF pretreatment plant for SWRO, Umm Lujj, Saudi Arabia)* [5].

In the first case, we present only a feasibility study because a full scale plant has not yet been built. In the second, we show that the *NanoFlux* predictions are in good agreement with the real plant operating data. It is thus possible to obtain quick and reliable simulation results thanks to both the powerful and robust computational algorithms employed and the internal *NanoFlux* database that contains the principal commercial membranes. This modeling tool is easy to use, thanks to its ergonomic

graphical user interface, and has been validated using real case studies [1–3].

There is a pressing need for simulation tools in NF because the complexity of the transport mechanisms, coupled with the wide range of different nanofilters and plant designs available, makes it extremely difficult to choose the right membrane and plant design for a given application in a reliable and cost effective way [6–8]. Reliable transport modeling is especially crucial in this area because the composition of the permeate (the product) depends sensitively on the choice of membrane, the pH and composition of the feed (individual ionic concentrations and total feed ionic strength) and the operating conditions (applied pressure, cross-flow velocity, etc.). Since in NF plants many membrane modules may be linked in series (Fig. 1), it is important for reliable plant simulations to be able to account for the changing feed composition and flux that is injected into each membrane element and the concomitant change in membrane performance (typically the feed gets more and more concentrated in proceeding from one element to the next in a brine-staged plant and the membrane rejection performance gets degraded). In order to gauge the global filtration performance and economic attractiveness of a plant design, reliable methods are also needed to model concentration polarization and tangential module pressure drops (the latter implies that

\*Corresponding author.

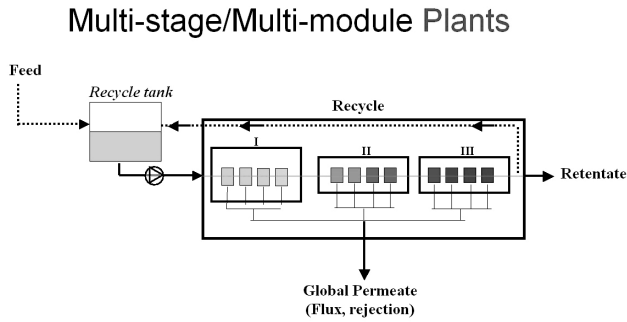


Fig. 1. Schematic diagram of a multi-stage/multi-module three brine-staged NF plant with each stage containing one housing composed of four membrane elements in series. In order to increase the plant productivity (total permeate flux) part of the retentate can be recycled and this feature can easily be handled with NanoFlux. The increasingly dark shade of each successive membrane element represents the increasing salt concentration.

the trans-membrane pressure for a given element, which is the transport driving force in NF, decreases as the feed passes from one element to the next).

Our results show that is feasible to use advanced membrane transport modeling techniques to perform reliable NF plant modeling for highly concentrated feeds in real-world applications (where a partial demineralization must often be carried out in situations where the composition and characteristics of the feed may change due to wide seasonal variations in salinity and/or temperature). The NanoFlux software tool puts the full power of state-of-the-art NF membrane transport modeling at the fingertips of plant engineers and ultimately decision-makers. The possibility of performing reliable simulations of plant performance sets the stage for reliable estimates of plant construction and operating costs.

## 2. Industrial applications of NF

For certain industrial applications, NF membrane processes have a number of advantages with respect to Reverse Osmosis (RO) ones [3–8]:

1. Lower working pressures and higher fluxes, leading to lower operating costs.
2. High rejection of organic molecules with molecular weights higher than the cut-off (MWCO) of the NF membrane (200–1000 Da) with potentially less fouling.
3. High rejection of multivalent ions and low to moderate rejection of monovalent ions, leading to a high *mono to multivalent selectivity*.

In industrial effluent and wastewater treatment one is usually concerned with reducing (in the filtration permeate) the concentration of: **organic compounds**, measured, for example, by COD (Chemical Oxygen Demand); **salts**,

but maintaining a high mono to multivalent ion selectivity; and **heavy metal ions**, all the while maintaining high permeate fluxes at relatively low working pressures and respecting environmental norms concerning the usually highly concentrated retentate. When NF is used as a pretreatment to a SWRO [5, 6] desalination plant, then the goal is to reduce the TDS (total dissolved solids), hardness, and turbidity sufficiently to take the load off the RO membranes and increase the recovery and lower the operational costs of potable water production.

## 3. Ion membrane transport and multi-scale plant modeling

The composition of the feed is fixed by the concentration of the  $N$  ions making up the mixture, each with a concentration  $c_i^f (i=1, \dots, N)$ . At the one membrane element level theoretical ion rejection predictions for multi-electrolyte solutions are obtained using a Hindered Electro-Transport (HET) theory that is based on the volume averaged Stokes equation for solution flow and incorporates steric and hydrodynamic hindrance factors into the Extended Nernst–Planck (ENP) ion flux equations and steric/Donnan partitioning at the membrane/solution interfaces [1–3, 8, 9]. The volume averaged Stokes equation is given by [3]

$$\frac{1}{L_p^0} j_v = -\partial P / \partial x - \rho \partial \phi / \partial x \quad (1)$$

and the ENP equations, which describe the coupled transport of  $N$  ions, are composed of three terms (diffusion, electrical migration, and convection) [3]:

$$j_i = -\bar{D}_i \frac{\partial \bar{c}_i}{\partial x} - z_i \bar{D}_i \bar{c}_i \frac{F}{RT} \frac{\partial \phi}{\partial x} + K_i^c \bar{c}_i j_v \quad (2)$$

The volume averaged Stokes equation (1) allows one to calculate  $j_v$  as a function of  $\Delta P$ , which requires  $L_p^0$  [m/(s Pa) or L/(h m<sup>2</sup> bar)], the pure water hydraulic permeability. The other quantities and parameters appearing in Eqs. 1 and 2 are :

$j_i$	molar ionic flux density (mol m <sup>-2</sup> s <sup>-1</sup> ),
$\bar{D}_i$	effective ionic diffusion coefficient in the membrane (m <sup>2</sup> s <sup>-1</sup> ),
$\bar{c}_i(x)$	local average ionic concentration in the membrane (moles/m <sup>3</sup> of pore volume),
$P(x)$	local average pressure in the membrane (bar),
$\phi(x)$	local average electrical potential in the membrane (V),
$j_v$	trans-membrane solution volume flux density (m s <sup>-1</sup> or L h <sup>-1</sup> m <sup>-2</sup> ),
$x$	transverse distance across the membrane (m) ( $0 \leq x \leq l_m$ , where $l_m$ is the membrane thickness).

In Eq. 1  $\rho(x) = F \sum_i z_i \bar{C}_i(x)$  is the local ion charge density. In Eq. 2,  $K_i^c$  is the convective hindrance factor and the effective ionic diffusion coefficients,  $\bar{D}_i$ , can be written as,  $\bar{D}_i = D_i K_i^d \phi_p / \tau$ , where  $D_i$  is the bulk ionic diffusion coefficient,  $K_i^d$  is the hindered diffusion factor,  $\phi_p$  is the membrane porosity, and  $\tau$  is the effective tortuosity. It is thus possible to define an effective membrane thickness,  $l_{eff} = (l_m \tau) / \phi_p > l_m$ . The dimensionless convective and diffusive hindrance factors,  $K_i^c$  and  $K_i^d$ , depend on  $\lambda_i = r_i / r_p$ , the ratio of the ionic radius,  $r_i$ , to the effective membrane pore radius,  $r_p$  (some of the ion parameters used in the NanoFlux simulations are collected in Table 1). Furthermore, in NF, the electric current density across the membrane vanishes,  $j_c = F \sum_{i=1}^N z_i j_i = 0$ , which allows one to obtain a relation between the electric potential gradient and the ionic concentrations. At the macroscopic level electro-neutrality must be obeyed in the feed, membrane and permeate:

$$\begin{aligned} \sum_{i=1}^N z_i c_i^f &= 0 \quad (\text{feed}); \quad \sum_{i=1}^N z_i \bar{C}_i(x) + X_m = 0 \quad (\text{membrane}); \\ \sum_{i=1}^N z_i c_i^p &= 0 \quad (\text{permeate}) \end{aligned} \quad (3)$$

where  $c_i^f$  and  $c_i^p$  are, respectively, the ionic concentrations in the feed and the permeate and  $X_m$  is the effective membrane charge (moles/m<sup>3</sup> of pore volume). In NF the HET equations must be solved using the filtration condition  $c_i^p = j_i / j_v$ , as well as Donnan/steric partitioning at the membrane/external solution interfaces. An extended version of the transport model has been developed for modeling the NF of highly concentrated feeds. In this extended model a residual partition coefficient,  $k_i^{res}$ , is introduced into the ion partition coefficients,  $k_i$ , for certain ionic species in order to account for exclusion effects other than the electrostatic and steric ones (dielectric,...) [10–14]:

$$k_i^{(p)} = \frac{\bar{C}_i^{(p)}}{c_i^{(p)}} = k_i^{res} \Phi_i^s \exp \left[ - \frac{z_i F}{RT} \Delta \phi_D^{(p)} \right] \quad (4)$$

Table 1  
Ion parameters used in the NanoFlux simulations.

Ion	Bulk diffusion coefficient (10 <sup>-9</sup> m <sup>2</sup> .s <sup>-1</sup> )	Crystal (Pauling) radius (nm)
Na <sup>+</sup>	1.334	0.095
K <sup>+</sup>	1.957	0.133
Ca <sup>2+</sup>	0.792	0.099
Mg <sup>2+</sup>	0.706	0.065
Cl <sup>-</sup>	2.032	0.181
HCO <sub>3</sub> <sup>-</sup>	1.185	0.207
SO <sub>4</sub> <sup>2-</sup>	1.065	0.290

where the second term,  $\Phi_i^s$ , accounts for steric effects and the last for electrostatic (Donnan) ones [ $\Delta \phi_D^{(p)}$  is the Donnan potential at the feed (f) (permeate (p)) interfaces].

Once the filtration problem has been well defined, **NanoFlux** can be used to calculate numerically (via accurate and robust finite difference methods) all the interesting system properties, including ionic rejection  $R_i = 1 - c_i^p / c_i^f$  and volume flux density,  $j_v$ , vs. applied pressure,  $\Delta P$ , and the filtration potential  $\Delta \phi_f$  (or any of its components, such as the streaming potential). The parameters that must be supplied in order to perform rejection and potential calculations are :

- $c_i^f$ , ionic feed concentrations [mol/m<sup>-3</sup> or mol/L<sup>-1</sup>],
- $r_i$ , the effective ion radii [m],
- $r_p$ , the effective membrane pore radius [m],
- $l_{eff}$ , the effective membrane thickness [m],
- $X_m$ , effective membrane charge density [mol m<sup>-3</sup> or mol/L<sup>-1</sup>].

For the effective ion size we have chosen to adopt the ion crystal (or Pauling) radius, which, although certainly an approximation in an aqueous medium, has been shown to be a reasonable starting point for explaining differences in rejection between ions of the same valence [1–3, 9]. The membrane parameters,  $r_p$ ,  $l_{eff}$  and  $X_m$ , are termed “effective” because their chosen values are based on an approximate modeling protocol—and not an *ab initio* approach—that depends on fitting the model to experiment (the chosen values do not therefore necessarily correspond to the “real” physical values). The extended transport model also requires the residual ionic partition coefficients, which are estimated by fitting the transport model to single salt rejection experiments at high feed concentrations where all electrostatic effects are strongly screened and can therefore to a very good approximation be neglected.

#### 4. NF single element and plant simulation

In order to simulate the operation of real NF plants several hurdles had to be overcome, including the ability to handle:

1. Multi-component ion mixtures (~ 7 predominant ones in seawater and effluents);
2. Multiple modules and/or Multiple-stages;
3. Concentration polarization effects;
4. Tangential pressure drops (cross-flow hydrodynamics).

As we demonstrate here, **NanoFlux** meets these requirements and can therefore be used for modeling R&D and industrial applications of NF (for feeds possessing up to eleven ions). The ion transport equations

are solved across each membrane element and mass and flow balance is imposed within each membrane module. Trans-membrane transport and mass and flow balance equations are coupled to each other and therefore they must be solved iteratively in order to obtain a self-consistent numerical solution to the multi-scale NF transport problem (from the active NF layer up to the full multi-stage/multi-module plant, see Fig. 1). The model membrane parameters (Eq. 4) used in the transport modeling, which depend in general on feed pH and ionic concentrations, are drawn from the internal NanoFlux “membrane-single salt” database [1–3]. The database values of these membrane parameters ( $X_m$  and  $l_{eff}$ ) for a single salt-membrane pair are obtained by adjusting the HET model to experimental salt rejection data, obtained at carefully chosen values of feed salt concentration and pH. Estimates for the model membrane parameters for both single salts and ion mixtures (containing up to 11 ions) in conditions not studied experimentally are obtained using robust interpolation, extrapolation, and weighting methods [1–3, 12]. If the physical membrane thickness,  $l_m$ , can be measured using electron microscopy, then the fitted value for  $l_{eff}$  can be used to estimate the combined effects of tortuosity and porosity:  $l_{eff}/l_m = \tau/\phi_p$ . In membrane filtration, the ionic concentrations,  $c_i$ , and fluxes,  $Q$ , for the feed ( $f$ ), permeate ( $p$ ), and retentate ( $r$ ) are related via single element/module mass and flow balance ( $c_i^f Q_f = c_i^p Q_p + c_i^r Q_r$ ,  $Q_f = Q_p + Q_r$ ). The driving force is the average pressure gradient across the membrane; the volume flux density,  $j_v$ , crossing the membrane increases with increasing pressure and the ion rejection,  $R_i$ , is a function of  $j_v$ .

The best choice of NF membrane and plant design depends on the feed flux and composition and on the **target goals** for the **productivity** (permeate flux) and **retentate flux**, as well as the **quality** of the **permeate** and **retentate** in terms of component concentrations. The major challenge of designing an NF plant for a given industrial problem is to arrive at the imposed productivity and quality targets accurately and at the lowest possible cost. An important result of an extensive study of NF membranes suitable for use in a pre-treatment plant for SWRO [6] was that at the high TDS typical of seawater, NF membranes can be divided roughly into three groups with very different filtration performances: **group 1** membranes have high rejection and low permeate flow; **group 2** membranes have an intermediate balanced performance of permeate flow and ion rejection; and **group 3** membranes have high flow and modest rejection. Faced with this variety, the goal of **NF process modeling** is to speed-up both the choice of membrane and plant design, as well as plant operating optimization, using suitable simulation tools, such as *NanoFlux*.

#### 4.1. NF of brackish and highly concentrated brines (textile effluent, Tunisia)

We first perform trial NanoFlux simulations for a tertiary membrane treatment of a textile wastewater from a Tunisian dyeing, gluing and finishing factory specialized in denim fabric [4]. For purposes of illustration and to test the feasibility of using NF, we model the ionic rejection performance of a large scale plant equipped with the GE-Osmonics **DesalDK-8040** NF membrane, the goal being to reduce the TDS and hardness down to factory constraint levels, thereby allowing the reuse of the water in the process. The feed used in NF plant simulations is given in Table 2. With a MWCO of 200–300 Da (and an effective pore radius of about 0.44 nm) the DesalDK membrane can be considered to be an intermediate (group 2) nanofilter as far as pore size and effective membrane charge density go (according to the above classification). (The effective pore radius was obtained using NanoFlux by fitting the hindered transport model to experimental rejection data obtained for model neutral solutes [14]).

Before presenting simulation results for the full scale plant, we show in Figs. 2 (a) and (b) the Permeate volume flux density (a) and Ionic rejection (b) vs. Applied trans-membrane pressure for a single DesalDK membrane element. We note in Fig. 2 that the predicted volume flux density for the NF feed defined in Table 2 is substantially lower than that obtained for pure water (a result of osmotic pressure and electroviscous effects). We also note that above an applied pressure of about 12 bar [or permeate volume flux density of about 30 L/(h m<sup>2</sup>)], the ionic rejections reach plateau values with the following characteristics: the monovalent anions have moderate to high rejections (60 and 80% for Cl<sup>-</sup> and HCO<sub>3</sub><sup>-</sup>, respectively), the monovalent cations have high rejections (around 85% for Na<sup>+</sup> and K<sup>+</sup>), and the divalent ions have very high rejections (greater than 98% for Ca<sup>2+</sup>, Mg<sup>2+</sup>, and SO<sub>4</sub><sup>2-</sup>). Although the single membrane element simulations

Table 2

Ionic composition of the textile effluent feed for the NF plant (7 ions: 4 cations and 3 anions); total ionic strength of the NF feed, 0.136 mol/L; TDS 7.5 g/l [4].

Ion	mg/L	mol/L
Na <sup>+</sup>	2340	0.09990
K <sup>+</sup>	95.4	0.00240
Ca <sup>2+</sup>	30.0	0.00074
Mg <sup>2+</sup>	11.0	0.00044
Cl <sup>-</sup>	680	0.01953
SO <sub>4</sub> <sup>2-</sup>	2790	0.02957
HCO <sub>3</sub> <sup>-</sup>	1560	0.02603
<b>Total</b>	<b>7500</b>	

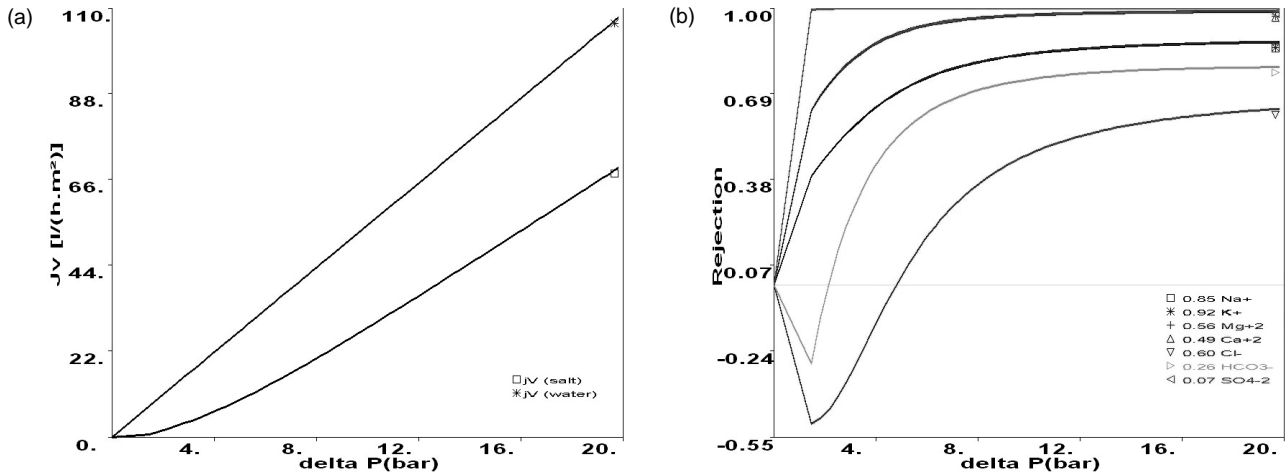


Fig. 2. NanoFlux simulations for the Textile effluent feed (a) Permeate volume flux density and (b) Ionic rejection versus applied trans-membrane pressure for a single DesalDK membrane element (30°C, pH 8, NF feed solution defined in Table 2). Negatively charged membrane with  $X_m = 0.16 \text{ mol/L}$  and  $l_{\text{eff}} = 30 \text{ }\mu\text{m}$  (obtained from the NanoFlux internal database).

give an idea of how well an NF plant equipped with this membrane could perform, they are not sufficient for a full understanding because of the changing nature of the feed injected into each successive element in a multi-module plant. For this reason we now turn to the NF plant simulations.

For illustrative purposes we fix the incoming feed flux at  $Q_f = 98 \text{ m}^3 \text{ h}^{-1}$  ( $98\,000 \text{ L h}^{-1}$ ) and adopt the following plant design: 8" membrane elements with six elements in series per housing arranged in a 3-brine staged 6:5:4 configuration without recycling (six housings in parallel in stage 1, five in parallel in stage 2, and four in parallel in stage 3). There are 90 membrane elements in this plant. Because in a brine staged set-up the retentate of one stage becomes the feed of the next, very high yields  $Y$  can be reached for large plants, even without recycling [ $Y = (\text{Permeate Flux})/(\text{Feed Flux})$ ]. The total membrane surface area is  $S_{\text{total}} = 2927 \text{ m}^2 = 90 \text{ membrane elements} \times 32.52 \text{ m}^2/\text{element}$ .

The results of the simulations, which are presented in the NanoFlux panel, Fig. 3, suggest that the present NF plant is capable of reducing the salt concentration and hardness to low enough levels for the reuse of the water in the industrial process. The predicted permeate flux, coming from combining the permeates of the 3 stages, is  $Q_p = 87.5 \text{ m}^3 \text{ h}^{-1}$  ( $87\,500 \text{ L h}^{-1}$ ). The retentate flux is  $Q_R = 10.5 \text{ m}^3 \text{ h}^{-1}$  ( $10\,500 \text{ L h}^{-1}$ ) and the global yield is  $Y = Q_p/Q_f = 89\%$ . In the simulation the feed pressure of 20 bar was chosen to get a yield close to 85%. An overall measure of productivity per unit feed pressure and unit membrane surface area is the global permeability:  $L = Q_p/(P_{\text{Feed}} S_{\text{total}}) = 1.5 \text{ L}/(\text{h m}^2 \text{ bar})$  [to be compared with the pure water permeability of  $4.87 \text{ L}/(\text{h m}^2 \text{ bar})$ ]. The permeate TDS is  $2.68 \text{ g L}^{-1}$  and that of the retentate is  $48.13 \text{ g/L}$ . Although the global ion TDS rejection is 65% (72% in terms of ionic strength),

the value for monovalent ions is much lower than that for divalent ones ( $> 90\%$ ), leading to high multi- to monovalent ion **selectivity**, as expected in NF. The ratio of mono to multivalent ion concentrations has thus greatly increased in going from the feed to the permeate, thanks to the very high rejection of multivalent ions. On the contrary this ratio has decreased in going from the feed to the retentate, as follows from simple mass balance. For each stage the following detailed individual stage information can be read off the results panel (Fig. 3):

Membrane Surface [m <sup>2</sup> ]	Permeate volume flux density $J_v$ [L/(h m <sup>2</sup> )]
Permeate Flux, $Q_{p,\text{stage}}$ [L h <sup>-1</sup> ]	Retentate Flux, $Q_{R,\text{stage}}$ [L/h]
Stage Yield (Recovery), $Y = Q_{p,\text{stage}}/Q_{f,\text{stage}}$	Average Pressure drop $\Delta P$ [bar]

For each ion the following simulation results are also presented: Feed, Permeate, and Retentate concentrations [mol L<sup>-1</sup>]; Ion passage,  $T_i = c_i^p / c_i^f$  [-], Ion rejection,  $R_i = 1 - T_i$  [-], and Ion removal =  $Q_R \times c_i^r$  [mol h<sup>-1</sup>]. An important factor, besides the quality of the permeate (controlled by the ion passage or rejection), is the **retentate concentration factor**  $RCF_i = c_i^r / c_i^f$ , which can be obtained from the results panel (Fig. 3). When it comes to evaluating methods of retentate disposal, this factor is especially important for certain multivalent ions, because of precipitation thresholds or high toxicity (such as for heavy metal ions, if present). In the present case the NanoFlux predictions reveal that the retentate is 6 times more concentrated than the feed in terms of TDS.

The details concerning the changes in ionic concentrations as one progresses through each of the three stages can also be obtained using NanoFlux. These

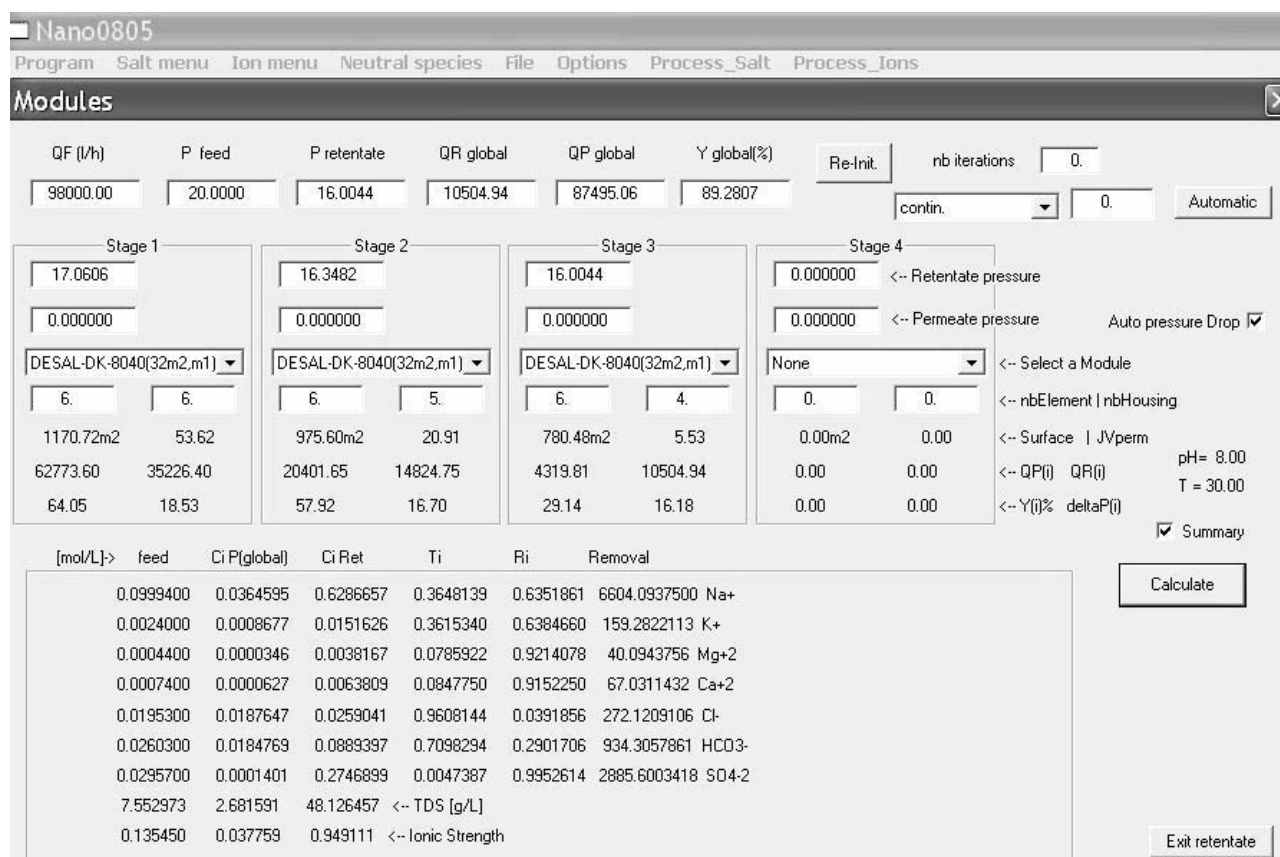


Fig. 3. NanoFlux “configuration and results” panel for a brine-staged 6:5:4 plant and textile effluent feed (Table 2); Feed flux, QF, is 98 m<sup>3</sup>/h and the applied feed pressure is P<sub>feed</sub> = 20 bar.

simulation results, which are presented in Table 3, illustrate one of the main characteristics of NF, namely that the ionic feed concentrations entering each successive stage (= retentate concentrations of the previous stage) are almost always increasing (due to ion rejection) and therefore the performance of each stage in terms of rejection and flux go down. Further NanoFlux simulations can easily be carried out using other plant designs and other NF membranes (for example, the choice of a

looser NF membrane might be better in terms of cost effectiveness, i.e., higher productivity at lower pressure, all the while meeting the product constraints). In this way a comparative membrane and plant design study can be made via computer simulations even before performing time-consuming and costly pilot studies. It will be interesting to compare the results of the NanoFlux simulations with pilot studies, as well as full-scale plant operating data, if and when they become available.

Table 3

Stage-by-stage ionic concentrations [mol/L] for the 6:5:4 plant and textile effluent feed (Table 2).

[mol/L] Feed	Stage 1		Stage 2		Stage 3		Permeate global	
	perm	Reten/Feed	perm	Reten/Feed	perm	Reten/Feed		
Na <sup>+</sup>	0.09994	0.01966	0.24300	0.06229	0.49168	0.15857	0.62867	0.03646
K <sup>+</sup>	0.00240	0.00046	0.00585	0.00149	0.01185	0.00381	0.01516	0.00087
Mg <sup>+2</sup>	0.00044	0.00001	0.00121	0.00006	0.00278	0.00027	0.00382	0.00003
Ca <sup>+2</sup>	0.00074	0.00002	0.00202	0.00011	0.00466	0.00046	0.00638	0.00006
Cl <sup>-</sup>	0.01953	0.01120	0.03438	0.03301	0.03625	0.06142	0.02590	0.01876
HCO <sub>3</sub> <sup>-</sup>	0.02603	0.00888	0.05659	0.03066	0.09227	0.10036	0.08894	0.01848
SO <sub>4</sub> <sup>-2</sup>	0.02957	0.00005	0.08217	0.00022	0.19495	0.00103	0.27469	0.00014

4.2. Seawater NF (NF pretreatment plant for SWRO, Umm Lujj, Saudi Arabia)

The use of NF to desalinate brackish and sea water is the object of several important ongoing investigations [5–7, 15–17]. We carry out NanoFlux simulations first at the single element level and then for the full scale Umm Lujj SWNF plant, built with the DesalDK membrane to be used as a pre-treatment step for the SWRO of Red seawater feed given in Table 4. The model predictions are then compared with the plant operating data presented in [5]. The choice of NF membrane for this SWRO pretreatment application, which was made after a long and extensive pilot level study [6], was dictated by the following criteria: (1) prevent RO membrane fouling by prior turbidity and bacteria removal, (2) prevent scaling by prior removal of divalent hardness ions, (3) reduce the TDS load on the SWRO plant in order to lower RO operating pressures and increase product yield. Before presenting the full scale plant

simulations, we compare the Nanoflux predictions for the DesalDK membrane and the Red Seawater feed (Table 4) with those obtained above for the textile effluent feed (Table 2): by comparing Fig. 2 with Fig. 4 we note that for the Red Seawater feed, which is about six times more concentrated than the textile effluent one, (i) the predicted permeate flux density at an applied pressure of 20 bar is about two times lower than for the textile effluent feed, (ii) the predicted monovalent ion rejections are, aside from  $\text{HCO}_3^-$ , about two times lower at 20 bar ; (iii) the predicted monovalent cation rejections are slightly negative at low pressure in contrast to what is obtained for the textile effluent feed, for which the monovalent cation rejections remains positive and the monovalent anion rejections are strongly negative at low pressure; and (iv) the predicted divalent ion rejections remain high, despite the much higher feed TDS.

The actual SWNF plant consists of one stage composed of 27 housings in parallel with each housing

Table 4

Red Sea water ionic feed composition [5,6] used in the SWNF NanoFlux simulations and the measured and predicted ionic and TDS rejections (%). Total ionic strength of the NF feed, 0.83 mol/L; TDS 41 g/l.

Ion	mg/L	mol/L	Expt. Rejection	Simulations
Na <sup>+</sup>	12564	0.552	–	11
K <sup>+</sup>	397	0.010	–	14
Mg <sup>2+</sup>	1595	0.065	98	98
Ca <sup>2+</sup>	477	0.011	92	93
Cl <sup>-</sup>	22969	0.647	24	23
HCO <sub>3</sub> <sup>-</sup>	157	0.003	44	47
SO <sub>4</sub> <sup>2-</sup>	3227	0.033	>99	99
TDS	41 400		28	29

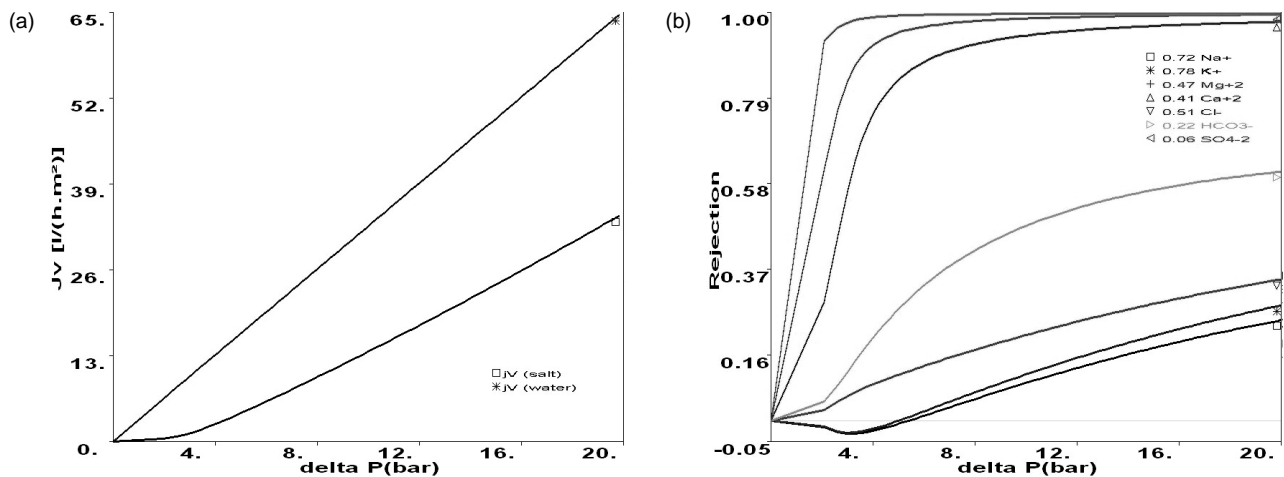


Fig. 4. NanoFlux simulations for the Red Seawater feed (a) Permeate volume flux density and (b) Ionic rejection vs. Applied trans-membrane pressure for a single DesalDK membrane element (23° C, pH 6.7, NF feed solution defined in Table 4). Negatively charged membrane with  $X_m = 0.33$  mol/L and  $l_{eff} = 18.5 \mu\text{m}$  (obtained from the NanoFlux internal database).

containing six 8" DesalDK-8040F elements. The total effective membrane surface area is about 5270 m<sup>2</sup>. The feed flux is fixed at 360 m<sup>3</sup> h<sup>-1</sup> (360 000 L h<sup>-1</sup>), the feed pH at 8.2, the temperature at 32°C, and the applied feed pressure is 25 bar. The results of the simulations, which are presented in the NanoFlux panel, Fig. 5, show very good agreement with the actual plant operating data (Table 4).

The measured and predicted yields are 65 and 71%, respectively, and the measured and predicted TDS rejections are 28 and 29%. We also observe in Table 4 that the NanoFlux results for the ionic rejections are in good agreement with the plant operating data, especially the very high measured and predicted divalent ion rejections, which range between 92 and 99%. In view of the relatively low TDS rejection, which is dominated by the monovalent ion contribution, it is also clear why a group 2 type NF membrane, such as the DesalDK, is suitable to be used in an NF pretreatment plant for SWRO, but not for the production of potable water directly.

## 5. Conclusions

The results presented here show that NanoFlux can be a useful tool for carrying out feasibility studies and for designing NF plants. Furthermore, the good agreement between the actual *Umm Lujj* SWNF operating data and the plant simulations reveals that NanoFlux can provide a fast and reliable way of modeling desalination via NF. In view of the increasing importance of finding economical ways of producing recyclable and potable water in a period of ongoing shortages, the improved design and optimization of nanofiltration plants via process simulation tools should become a crucial step in the implementation of NF membrane technology.

## Acknowledgements

Work supported in part by the French ANR Program NANO-2007, Project SIMONANOMEM.

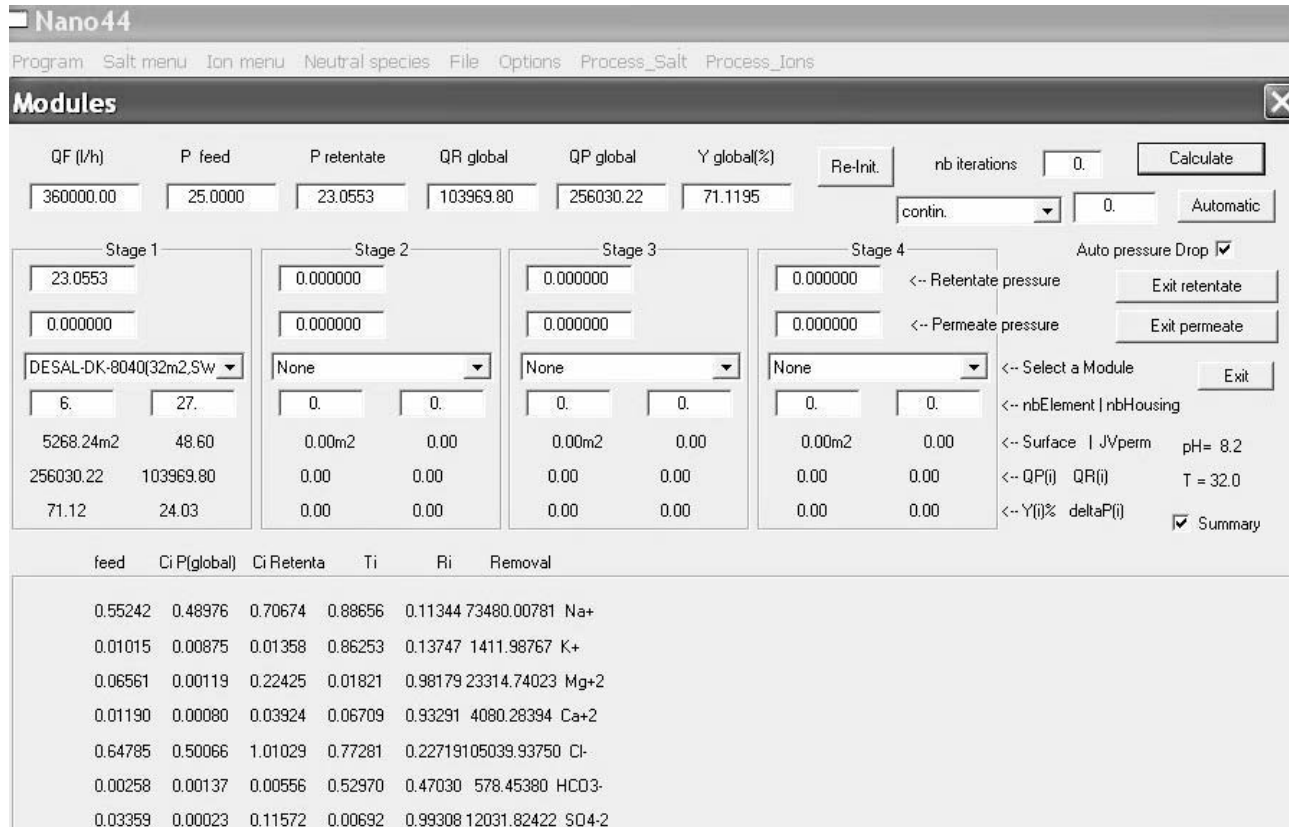


Fig. 5. NanoFlux “configuration and results” panel for the single stage NF plant used as pretreatment for the SWRO of Red Seawater feed presented in Table 4; Feed flux, QF, is 360 m<sup>3</sup>/h and the applied feed pressure is P<sub>feed</sub> = 25 bar.

## References

- [1] J. Palmeri, et al. *Desalination*, 147 (2002) 231.
- [2] X. Lefebvre, et al. *Sep. Purif. Technol.*, 32 (2003) 117.
- [3] H. Chmiel, X. Lefebvre, V. Mavrov, M. Noronha, J. Palmeri, Computer Simulation of Nanofiltration, Membranes and Processes, In: M. Rieth and W. Schommers (Eds.), Handbook of Theoretical and Computational Nanotechnology, Volume 5, American Scientific Publishers, 2006, pp. 93–214.
- [4] N. Ben Amar, N. Kechaou, J. Palmeri, A. Deratani, A. Sghaier, *J. Hazard. Mater.*, 170 (2009) 111.
- [5] P. Eriksson, M. Kyburz, W. Pergrande. *Desalination*, 184 (2005) 281.
- [6] A. M. Hassan, et al. *Desalination*, 131 (2000) 157.
- [7] S. Adham, S. R. C. Cheng, D. X. Vuong, K. L. Wattier. *The International Desalination & Water Reuse Quarterly*, 13 (3) (2003) 18.
- [8] W.R. Bowen and A.W. Mohammed. *Trans IChemE, A* 76, (1998) 885.
- [9] X. Lefebvre, J. Palmeri, P. David. *J. Phys. Chem.*, B 108 (2004) 16811.
- [10] G. Hagemeyer and R. Gimbel, *Desalination*, 117 (1998) 247.
- [11] A. Yaroshchuk, *Adv. Colloid Interface Sci.*, 85 (2000) 193.
- [12] X. Lefebvre, Ph.D. thesis (in French), *Etude des modèles de transfert en nanofiltration. Application du modèle hybride basé sur les équations de Nernst-Planck étendues par le développement du logiciel de simulation "Nanoflux"*, University of Montpellier 2, France (2003).
- [13] A. Szymczyk and P. Fievet, *J. Membr. Sci.*, 252 (2005) 77.
- [14] W. R. Bowen and J.S. Welfoot, *Chem. Eng. Sci.*, 57 (2002) 1121.
- [15] C. Oumar-Anne, D. Trebouet, P. Jaouen, F. Quemeneur. *Desalination*, 140 (2001) 67.
- [16] M. Pontié, et al. *Desalination*, 158 (2003) 277.
- [17] R. Haddad, E. Ferjani, M. S. Roudesli, A. Deratani. *Desalination*, 167 (2004) 403.